Joint Communication and Computation Resource Optimization in FD-MEC Cellular Networks

FANGNI CHEN [1,2], **(Member, IEEE), JIAFEI FU** [2]**, ZHONGPENG WANG** [1]**,**
YANG ZHOU [1]**, AND WEIWEI QIU** [1]

[1]School of Information and Electronic Engineering, Zhejiang University of Science and Technology, Hangzhou 310012, China
[2]College of Information Engineering, Zhejiang University of Technology, Hangzhou 310012, China

Corresponding author: Fangni Chen (cfnini@zust.edu.cn)

ABSTRACT In view of the growing contradiction between the intensive computation demands and the resource limitations of mobile users, mobile edge computing (MEC) and simultaneous wireless information and power transfer (SWIPT) have emerged as new paradigms towards 5G communication. However, coordinating the communication and computation between users and edge servers proves to be challenging for MEC. In this paper, we propose a novel multi-user full-duplex (FD) communication system that combines MEC and SWIPT technology in order to take the advantage of high-speed mobile computing and long-lasting self-sustainability. Through MEC technology, users are able to calculate local computation tasks using their batteries, and can offload partial computation tasks to the base station (BS) to reduce their energy shortage. Moreover, users can refill their batteries while receiving the computation result sent by the BS, thus benefiting from SWIPT technology. The FD mode can potentially increase the system performance by allowing the simultaneous transmitting and receiving of computation tasks. Our work aims to minimize the energy consumption of the system, while formulating resource allocation as a joint non-linear optimization problem. We decouple the original non-convex problem into two subproblems and solve them using a proposed algorithm that applies group iterative optimization. Numerical results prove that the proposed algorithm is superior to other two comparison schemes and can significantly reduce the system energy consumption and the latency.

INDEX TERMS Full-duplex, mobile edge computing, offload, simultaneous wireless information and power transfer, group iterative optimization.

I. INTRODUCTION

The era of the Internet of Things (IoT) has brought about a dramatic surge in data. In 2016, Cisco reported that global mobile traffic will increase by more than seven times over the period of 2015-2020, while network connection speeds will almost quadruple by 2020. In addition, terminal connection types and service scenarios have also exhibited an exponential growth. Ultra-low delay and ultra-high efficiency, reliability and density connections have become necessary requirements of future mobile communication systems [1]–[3], while also accelerating the development and implementation of 5G systems [4]. Many new application scenarios have emerged, including artificial intelligence/virtual reality

(AR/VR) [5]–[7], automatic driving, industrial Internet, vehicle networking, smart cities, and smart agriculture [8], [9]. Therefore, a novel network framework and corresponding resource management scheme are urgently required to take on the rapid development in technology that is currently observed [10].

Since the limited computing capability of users does not generally match the explosion of data traffic, mobile edge computing (MEC) [11] has become an attractive scheme. MEC is regarded as a promising technology for computation-sensitive scenarios, as it enables mobile devices to offload their tasks to the edge cloud for processing. MEC plays an important role in quality of service (QoS), as it is particularly capable of significantly improving the latency performance of mobile devices when offloading computation tasks to the MEC server [12].

The associate editor coordinating the review of this manuscript and approving it for publication was Amjad Ali.

Moreover, with the rapid development of mobile device performance and computing loads, the energy consumption of mobile devices has significantly grown. In order to overcome such mobile device sustainability challenges, wireless energy harvesting (WEH) is proposed for the self-sustained communication through wireless charging [13]. Simultaneous wireless information and power transfer (SWIPT) [14] arose as a breakthrough technology that divides radio frequency (RF) signals into two parts, information transmission and energy collection, providing a feasible solution for excessive network energy consumption [15], [16]. SWIPT is able to apply two different receiver architectures; time switching (TS) periodically switches between information decoding (ID) and energy harvesting (EH), and power splitting (PS) simultaneously executes ID and EH [17].

Developed on the basis of high spectrum efficiency, full-duplex (FD) technology [18], which can transmit and receive information simultaneously, was introduced to extend the potential capabilities of devices. FD nodes support amplification and forwarding transmission technology, and can effectively improve communication capabilities without increasing memory occupation and latency [19], [20]. Strengthened by improvements of self-interference (SI) cancellation technology [21]–[23], the FD technology is widely applied in relay, small cellular networks (SCNs) and device-to-device (D2D) communications to ensure QoS [24], [25]. In the real communication environments, channels are time varying and wireless devices are not ideal. Thus, the application of FD technology with heterogeneous services in imperfect channels has attracted much attention for QoS [26].

In this paper, we investigate a multi-input multi-output (MIMO) [27] FD-enabled wireless communication system integrated with MEC and SWIPT technologies, which intend to meet the requirements of great computation capability, long battery lifetime, high spectral efficiency and low latency for the explosive expanding communications. Certain works [28]–[30] have started research on the related framework and they already proved that it is a feasible and practical solution to combine FD with MEC and SWIPT technology. To the best of our knowledge, jointly considering and managing the power control, computing offloading policies and resource allocation of our framework has not been the subject of research thus far. Moreover, determining the optimization of this complex resource allocation problem is highly challenging. The contributions of this paper are summarized as follows:

1) We design a novel MEC framework with a MIMO FD-enabled base station (BS) and several SWIPT-enabled mobile users. Mobile users can offload computation tasks to the MEC server implemented via the BS. The BS can receive the offloading tasks and transmit the computation results from the MEC server to other users simultaneously based on the FD technology. On receiving the computation result, the users will additionally receive information and harvest energy by using SWIPT technology.

2) We formulate a joint optimization problem where the transmitted power, the CPU frequency, the transmission rate, and the uploaded computation task size are taken into account. The problem aims to minimize the total system energy consumption over a time block while guaranteeing the QoS constraints of the system.

3) An efficient algorithm to solve the optimization problem is proposed. Since the original problem is non-convex, we transform it into two subproblems. The closed-form solution of the CPU frequency is obtained through local computing optimization of the first subproblem. In the second subproblem, we divide the variables into two groups and transform the non-convex optimization problem into the convex optimization problem, which can be solved using the classical interior point algorithm. Owing to this characteristic, an group iterative optimization is proposed to effectively solve this subproblem with low computation complexity.

4) Numerical results are determined under varying scenarios and parameters. Simulation results demonstrate that the proposed algorithm shows the best energy consumption and latency performance compared with the two bench schemes.

The remainder of our paper is organized as follows. Section II discusses related works on wireless powered MEC systems with the different technologies. Section III details the system model, and Section IV presents the algorithm used to determine the optimal solution of the problem model. Section V provides numerical simulation results and Section VI concludes our work.

II. RELATED WORKS

Wireless powered MEC systems have recently attracted much interest as a promising technology [31]. Due to its ability to prolong the system lifetime, EH has been combined with MEC to provide a sustainable computation process for users [32]–[34]. In order to tackle the explosive growth of data traffic, non-orthogonal multiple access (NOMA) [35] has been proposed to attain higher spectral efficiency. NOMA based MEC systems have been proposed whereby users offload computation tasks to the BS using NOMA, while the BS simultaneously decodes information in [36] and [37].

Moreover, as EH partially occupies non-negligible bandwidth, FD technology can combine WEH and MEC with NOMA to optimize the allocation of communication, computing and energy resources in the Internet of Things. In addition, relay technology [38] was widely applied to reduce the impact of transmission latency in both half-duplex (HD) and FD protocols. The FD protocol, which generally receives more attention due to its capability to simultaneously transmit and receive information, can be summarized as follows. During the uplink, after receiving the computation bits from the user with a beamforming filter, the relay transmits the computation tasks to the BS. Following the processing of the computation tasks, the user downloads the computation results and energy using SWIPT. The user then decodes information and collects energy through the power splitting (PS) receiver.

The software-defined virtual cellular network (SDVCN) has been defined as an extension in [39], [40]. Through different mobile virtual network operators (MVNOs), users can offload computation tasks to access points (BS with MEC servers) using three pathways: the direct transmission of computing tasks to the access point (AP), the transmission of computing tasks to the AP through relay, and the transmission of computing tasks to the AP through virtual users. These virtual users and relays work in full duplex mode.

Task offloading mechanism and resource allocation are crucial problems in MEC systems [41]. In [42], a joint optimization of computing mode selection and the system transmission time allocation were presented to achieve the maximal computation rate. The works shown in [43] considered a three-node MEC system and pursued a joint computation and communication cooperation approach. In [44], a multi-antenna NOMA-enabled computation task offloading scheme was proposed for multi-user MEC systems. A weighted sum energy consumption minimization problem was formulated to implement the communication and computation resources allocation in partial and binary offloading cases.

We share the similar reasonable framework with several aforementioned works. In [28], a FD-MEC system with NOMA and energy harvesting technology was considered. They aimed at minimizing the total energy consumption of the system via power control, time scheduling and computation capacity allocation. The work shown in [29] provided a novel energy-efficient scheduling in wireless powered FD-MEC systems. In [30], a MIMO FD relay based SWIPT-MEC system and an energy efficient problem were formulated to minimize the system energy consumption.

In summary, these studies essentially focused on how to improve the computation capability of mobile terminals, how to reduce energy consumption and how to improve spectral efficiency, with the ultimate goal of achieving maximum energy efficiency. Different from [28] and [29], we apply multiple antennas for the base station (BS), which can provide performance gain as we will discuss in Section V. Also, there is no relay node in our framework, which makes the offloading process and resource allocation totally different from [30]. Based on this, we propose a resource optimization for an architecture with a FD-MEC equipped BS and SWIPT equipped users. Simulation results demonstrate the advantage of our proposed algorithm both in energy consumption and latency.

III. SYSTEM MODEL

Consider a multi-user wireless powered FD-MEC system with K single-antenna users and a M-antenna BS, as shown in Fig. 1. Each user is equipped with a power splitting (PS) receiver and the BS integrated with a MEC server located in the wireless cellular network in proximity to mobile subscribers. As demonstrated in Fig. 1, the PS receiver can operate in both energy harvesting (EH) state and information
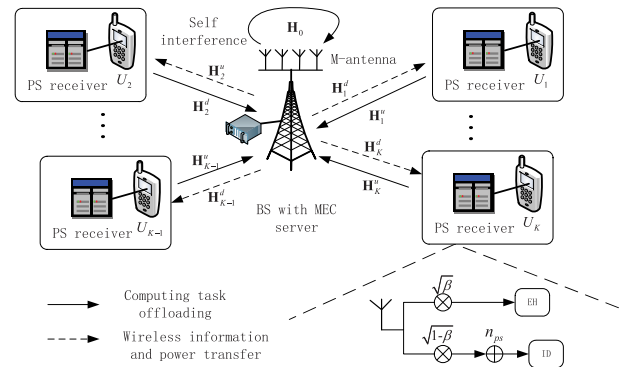

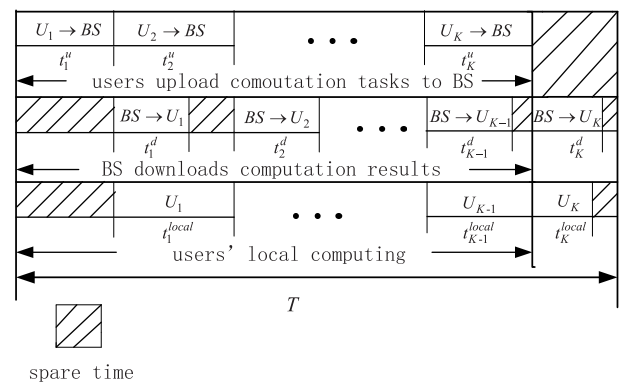**FIGURE 1.** System model of multi-user FD-MEC system.

FIGURE 2. The three system operation processes of the FD-MEC system.

decoding (ID) state, according to the conversion coefficient β ($0 \leq \beta \leq 1$).

As shown in Fig. 2, the time block with duration T is divided into K phases marked as t_i ($i \in \{1, \ldots, K\}, 0 \leq t_i \leq T$), whereby we assume that each computation task can be divided into two parts of arbitrary size by the user [45], and the computation task should be completed within each time block t_i. We set L_i as the total computation task size (in bits) of the user U_i, and L_i^u as the computation task size (in bits) that U_i uploads to the BS. Accordingly, $L_i - L_i^u$ represents the remaining computation bits executed locally, while L_i and L_i^u should satisfy

$$L_i^u = \alpha L_i, \tag{1}$$

where $0 \leq \alpha \leq 1$ is a weight factor. Based on the above settings, the three system operation processes are depicted in Fig. 2.

1) During the uplink process, U_i ($i \in \{1, \ldots, K\}$) uploads the computation task L_i^u to the BS. After receiving the computation bits, the MEC server deployed at the BS initiates computation of the task. Note that the computation latency is negligible due to the powerful computation capability of the MEC server.

2) During the downlink process, which has the same frequency as uplink, the BS simultaneously downloads the computation result L_j^r from the MEC server to the user

U_j ($j \in \{1, \ldots, K\}, j \neq i$). As soon as U_j receives the computation result, it will harvest energy and receive information from the radio frequency (RF) signal.

3) Local computing is performed by U_i during t_i^{local}.

These three processes will be described in more detail in the following analysis.

Rayleigh fading channel models are applied here, with channel coefficients from U_i to BS, and BS to U_i denoted as $\mathbf{H}_i^u \in \mathbb{C}^{M \times 1}$ and $\mathbf{H}_j^d \in \mathbb{C}^{1 \times M}$ respectively. The self-interference (SI) channel coefficient induced by the simultaneously transmission and reception of the BS is denoted as $\mathbf{H}_0 \in \mathbb{C}^{M \times M}$. In addition, $\mathbf{H}^u = [\mathbf{H}_1^u, \mathbf{H}_2^u, ..., \mathbf{H}_K^u]^T$, $\mathbf{H}^d = [(\mathbf{H}_1^d)^T, (\mathbf{H}_2^d)^T, ..., (\mathbf{H}_K^d)^T]^T)$. $(.)^T$ is the transposition operation.

A. UPLINK MODEL

In the uplink, users upload computation tasks to the BS in chronological order $\{U_1, U_2, ..., U_K\}$. Without loss of generality, during t_i^u, U_i uploads computation task L_i^u to the BS while the BS simultaneously downloads computation result L_j^r to U_j at the same frequency, where $i \in \{1, \ldots, K\}, j \in \{1, \ldots, K\}, i \neq j$. Hence, the received signal at the BS is as follows

$$\mathbf{y}_i^u = \sqrt{p_i^u}\mathbf{H}_i^u s_i^u + \mathbf{H}_0(\sqrt{p_j^d} s_j^d) + \mathbf{n_B}, \qquad (2)$$

where p_i^u is the uplink transmitted power of user U_i, which can be regarded as the transmit precoder of U_i. The uplink transmitted signal s_i^u and the downlink transmitted signal s_j^d are assumed with normalized power, which satisfy $|s_i^u|^2 = 1$ and $|s_j^d|^2 = 1$. $\mathbf{n_B} \in \mathbb{C}^{M \times 1}$ is the additive white Gaussian noise (AWGN) with power δ_B^2.

As shown in (2), the signal received at the BS consists of three components. The first component is the offloading task s_i^u transmitted by user U_i passing through the uplink channel $\mathbf{H}_i^u$. It is followed by the self-interference signal from the downlink transmission, whereby the computation result s_j^d from the BS to user U_j passes through the self-interference channel $\mathbf{H}_0$. The final component is the AWGN at the BS. Then, the received signal power at the BS and the signal to interference plus noise ratio (SINR) can be respectively expressed as:

$$\begin{aligned} P_i^u &= tr\{\mathbf{y}_i^u(\mathbf{y}_i^u)^H\} \\ &= p_i^u tr\{\mathbf{H}_i^u(\mathbf{H}_i^u)^H\} \\ &\quad + p_j^d tr\{\mathbf{H}_0\mathbf{H}_0^H\} + \delta_B^2 \\ &= p_i^u tr\{\mathbf{H}_i^u(\mathbf{H}_i^u)^H\} \\ &\quad + p_j^d tr\{\mathbf{H}_0\mathbf{H}_0^H\} + \delta_B^2, \end{aligned} \qquad (3)$$

$$SINR_{i,max}^u = \frac{p_i^u tr\{\mathbf{H}_i^u(\mathbf{H}_i^u)^H\}}{p_j^d tr\{\mathbf{H}_0\mathbf{H}_0^H\} + \delta_B^2}, \qquad (4)$$

where, $tr\{.\}$ is the operation of the matrix trace. Based on Shannon's theorem, the theoretical maximum achievable rate during the uplink transmission can be expressed as

$$R_{i,max}^u = Blog(1 + SINR_{i,max}^u), \qquad (5)$$

where B is the signal transmission bandwidth of the system. Let R_i^u represent the actual uplink transmission rate. As the actual uplink transmission rate can not exceed the theoretical maximum achievable rate $R_{i,max}^u$ [46], we can get

$$R_i^u \leq R_{i,max}^u. \qquad (6)$$

Accordingly, the latency of the offloading transmission is

$$t_i^u = \frac{L_i^u}{R_i^u}. \qquad (7)$$

Thus, the energy consumption at the offloading phase of U_i is expressed as

$$E_i^{off} = p_i^u t_i^u, \qquad (8)$$

and the energy consumption of all users can be derived as follows

$$E^{uo} = \sum_{i=1}^{K} p_i^u \frac{L_i^u}{R_i^u}. \qquad (9)$$

B. DOWNLINK MODEL

We denote p_j^d as the corresponding downlink transmitted power from the BS to U_j. The received signal at U_j is given as

$$y_j^d = \sqrt{p_j^d}\mathbf{H}_j^d s_j^d + n_j^d, \qquad (10)$$

where, n_j^d is the AWGN with power δ_j^2 at U_j.

Similar to the uplink transmission, the first component in (10) is the transmitted signal from the BS. For simplicity, any co-channel interference from the uplink to the downlink is neglected.

Accordingly, the received power at U_j is described as

$$P_j^d = p_j^d tr\{\mathbf{H}_j^d s_j^d (s_j^d)^H(\mathbf{H}_j^d)^H\} + \delta_j^2. \qquad (11)$$

For the received signal goes through PS receiver at U_j, β ($0 \leq \beta \leq 1$) portion is used for EH, while the remaining $(1-\beta)$ portion is used for ID. Thus, the harvest energy of all users can be written as

$$E^{uh} = \sum_{j=1}^{K} \beta P_j^d t_j^d, \qquad (12)$$

where t_j^d is the downlink transmission latency, expressed as

$$t_j^d = \gamma t_i^u, \qquad (13)$$

where $0 \leq \gamma \leq 1$ is a weight factor. (13) is reasonable because of the smaller size of downlink data and fast downlink transmission rate according to the practical applications. And the relationship between uplink transmission rate R_i^u and downlink transmission rate R_j^d is $\alpha R_i^u = \gamma R_j^d$.

Taking the sum of the energy consumption for each time slot at the BS, we obtain the energy consumption of the BS as follows

$$E^{BS} = \sum_{j=1}^{K} p_j^d t_j^d. \qquad (14)$$

C. LOCAL COMPUTATION MODEL

Denote t_i^{local} as the local computing latency, where $t_i^{local} \leq t_i^u$. Let C represent the CPU cycles required for computing 1-bit of data and f_i^n stands for the CPU frequency required for the $n-th$ CPU cycles, which satisfies

$$0 \leq f_i^n \leq f_i^{max}, \tag{15}$$

where f_i^{max} is the maximum CPU frequency. Thus, the corresponding computing latency is described as

$$t_i^{local} = \sum_{i=1}^{C(L_i-L_i^u)} \frac{1}{f_i^n}. \tag{16}$$

The local computing energy consumption can be derived as

$$E_i^{local} = \sum_{n=1}^{C(L_i-L_i^u)} \kappa(f_i^n)^2, \tag{17}$$

where κ is the effective capacitance coefficient based on the chip architecture of the user [47]. Therefore, the total local computation consumption is expressed as

$$E^{local} = \sum_{i=1}^{K} E_i^{local}. \tag{18}$$

D. PROBLEM FORMULATION

We aim to minimize the total energy consumption of the system, while ensuring that all computation tasks are completed. Based on (9), (12), (14) and (18), the total energy consumption of the system can be expressed as

$$E^{total} = E^{BS} + E^{uo} + E^{local} - E^{uh}. \tag{19}$$

Finally, we formulate the following joint optimization problem

$$(P1) \quad \min_{\mathbf{f}^n, \mathbf{p}^u, \mathbf{p}^d, \mathbf{L}^u, \mathbf{R}^u} E^{total}$$

$$s.t. \begin{cases} E^{uo} + E^{local} \leq E^{uh} \\ 0 \leq L_i^u \leq L_i \\ 0 \leq R_i^u \leq R_{i,max}^u \\ P_{min}^u \leq p_i^u \leq P_{max}^u \\ P_{min}^d \leq p_j^d \leq P_{max}^d \\ 0 \leq t_i^u, t_j^d \leq T \\ 0 \leq t_i^{local} \leq t_i^u \\ 0 \leq f_i^n \leq f_i^{max} \end{cases} \tag{20}$$

where $\mathbf{f}^n = [f_1^n, f_2^n, ..., f_K^n]$, $\mathbf{p}^u = [p_1^u, p_2^u, ..., p_K^u]$, $\mathbf{p}^d = [p_1^d, p_2^d, ..., p_K^d]$, $\mathbf{L}^u = [L_1^u, L_2^u, ..., L_K^u]$, $\mathbf{R}^u = [R_1^u, R_2^u, ..., R_K^u]$, $i \in \{1, ..., K\}, j \in \{1, ..., K\}$.

In problem $P1$, constraint 1) indicates that the users' energy consumption (local computing energy consumption plus offloading energy consumption) must not exceed their harvested energy. Constraints 2) and 3) imply that the offloading computation bits should not be greater than the total computation task bits, and that the actual achievable rate should

be no more than the maximum achievable rate respectively. Constraint 4) indicates that P_{min}^u and P_{max}^u are the lower and upper limits of each user's transmitted power. Similarly, constraint 5) denotes the power range transmitted by the BS. In constraint 6), the offloading latency of each user U_i and the downlink transmission time of the BS must not exceed the total time slot length T. In constraint 7), the local computing time should not exceed the uplink transmission time, while constraint 8) indicates that f_i^n should be below the maximum frequency, in according with (15).

IV. OPTIMAL SOLUTION

Due to the non-convexity of both the objective function and constraints, solving problem $P1$ proves to be highly challenging. Therefore, we divide the original problem P1 into two subproblems, local computation optimization and group iterative optimization. We first determine the optimal CPU frequency $\mathbf{f}^{opt}$ by local computation optimization and subsequently propose an iterative algorithm with low complexity for fixed $\mathbf{f}^n$. Since the variables $\mathbf{p}^u$, $\mathbf{p}^d$, $\mathbf{L}^u$ and $\mathbf{R}^u$ are coupled in the second subproblem, making the subproblem complex to solve, we adopt the method of group iterative optimization, where the first group of variables includes $\mathbf{p}^u$, $\mathbf{p}^d$ and $\mathbf{R}^u$, while the second group of variables includes $\mathbf{L}^u$ and $\mathbf{R}^u$.

A. LOCAL COMPUTATION OPTIMIZATION

In this section, we aim to optimize the CPU frequency $\mathbf{f}^n$. Inspired by [45], the optimal CPU frequency of each time block t_i should satisfy

$$f_i^1 = f_i^2 = ... = f_i^{C(L_i-L_i^u)} = f_i \tag{21}$$

where f_i represents the same CPU frequency maintained in each cycle. For the sake of brevity, let $\Gamma = E^{BS} + E^{uc} - E^{uh}$, then, the problem (P1) can be transformed into

$$(P1.1) \quad \min_{\mathbf{f}^n, \mathbf{p}^u, \mathbf{p}^d, \mathbf{L}^u, \mathbf{R}^u} \Gamma + \sum_{i=1}^{K} C(L_i - L_i^u)\kappa(f_i)^2$$

$$s.t. \begin{cases} E^{uo} + \sum_{i=1}^{K} C(L_i - L_i^u)\kappa(f_i)^2 \leq E^{uh} \\ 0 \leq L_i^u \leq L_i \\ 0 \leq R_i^u \leq R_{i,max}^u \\ P_{min}^u \leq p_i^u \leq P_{max}^u \\ P_{min}^d \leq p_j^d \leq P_{max}^d \\ 0 \leq t_i^u, t_j^d \leq T \\ 0 \leq \frac{C(L_i - L_i^u)}{f_i} \leq t_i^u \\ 0 \leq f_i \leq f_i^{max} \end{cases} \tag{22}$$

Clearly, in order to minimize the objective function, f_i has to be as small as possible. Thus, from the constraint $0 \leq \frac{C(L_i-L_i^u)}{f_i} \leq t_i^u$, we can determine the lower bound of f_i, the optimal CPU frequency, as follows

$$f_i^{opt} = \frac{C(L_i - L_i^u)}{t_i^u} \tag{23}$$

Algorithm 1 Local Computing Optimization

Input: $K, M, B, \mathbf{H}^u, \mathbf{H}^d, \mathbf{H}_0, T, C, \kappa, \beta, \gamma, \mathbf{L}, \delta_j^2, \delta_B^2, \mathbf{s}^u,$
$\quad \mathbf{s}^d, P_{min}^u, P_{max}^u, P_{min}^d, P_{max}^d, \mathbf{L}^u, \mathbf{p}^u, \mathbf{p}^d, \mathbf{R}^u$

1: According to (22), get the optimal CPU frequency $f_i^{opt} = \frac{C(L_i - L_i^u)}{t_i^u}$, and $t_i^{local} = t_i^u$

2: Convert (P1.1) into (P2) by putting $f_i^{opt} = \frac{C(L_i - L_i^u)}{t_i^u}$ and $t_i^{local} = t_i^u$ into P(1.1)

Output: $\mathbf{f}^{opt}$

Based on the above analysis, it is clear that, at each time block, we have $f_i^{opt} = f_i^1 = f_i^2 = ... = f_i^{C(L_i - L_i^u)} = \frac{C(L_i - L_i^u)}{t_i^u}$. By extending to K users, the optimal local energy consumption is executed through local computing at each time block. Now replace f_i^n with $\frac{C(L_i - L_i^u)}{t_i^u}$ in (16) and (17), we get

$$t_i^{local} = t_i^u \qquad (24)$$

$$E^{local} = \sum_{i=1}^{K} \frac{\kappa C^3 (L_i - L_i^u)^3}{(t_i^u)^2} \qquad (25)$$

Problem (P1.1) can now be rewritten as

$$(P2) \quad \min_{\mathbf{p}^u, \mathbf{p}^d, \mathbf{L}^u, \mathbf{R}^u} E^{total}$$

$$s.t. \begin{cases} E^{uo} + \sum_{i=1}^{K} \frac{\kappa C^3 (L_i - L_i^u)^3}{(t_i^u)^2} \leq E^{uh} \\ 0 \leq L_i^u \leq L_i \\ 0 \leq R_i^u \leq R_{i,max}^u \\ P_{min}^u \leq p_i^u \leq P_{max}^u \\ P_{min}^d \leq p_j^d \leq P_{max}^d \\ 0 \leq t_i^u, t_j^d \leq T \end{cases} \qquad (26)$$

This algorithm is depicted in **Algorithm 1**.

B. GROUP ITERATIVE OPTIMIZATION

In order to solve the non-convex problem (P2), we first convert it into the following equivalent problem

$$(P2.1) \quad \min_{\mathbf{p}^u, \mathbf{p}^d, \mathbf{L}^u, \mathbf{R}^u} \sum_{i=1}^{K} p_i^u t_i^u + \sum_{i=1}^{K} \frac{C^3 (L_i - L_i^u)^3}{(t_i^u)^2}$$

$$+ \sum_{j=1}^{K} p_j^d (\gamma t_i^u) - \sum_{j=1}^{K} \beta f(p_j^d)^d (\gamma t_i^u)$$

$$s.t. \begin{cases} \sum_{i=1}^{K} p_i^u t_i^u + \sum_{i=1}^{K} \frac{C^3 (L_i - L_i^u)^3}{(t_i^u)^2} \\ \leq \sum_{j=1}^{K} \beta f(p_j^d)(\gamma t_i^u) \\ 0 \leq L_i^u \leq L_i \\ 0 \leq R_i^u \leq R_{i,max}^u \\ P_{min}^u \leq p_i^u \leq P_{max}^u \\ P_{min}^d \leq p_j^d \leq P_{max}^d \\ 0 \leq t_i^u \leq T \end{cases} \qquad (27)$$

where $f(p_j^d) = P_j^d, f(p_j^d)$ is a linear function of p_j^d as (11). And since $t_j^d = \gamma t_i^u, 0 \leq \gamma \leq 1$, constraint $0 \leq t_i^u, t_j^d \leq T$ can be transformed into $0 \leq t_i^u \leq T$.

As problem (P2.1) is still a non-convex problem, we propose an asymptotic algorithm that divides all variables into two groups for iterative optimization. The first group is $(\mathbf{p}^u, \mathbf{p}^d, \mathbf{R}^u)$, while the second group is $(\mathbf{L}^u, \mathbf{R}^u)$. After optimizing the first set of variables, we bring the optimal solution to the second set of variables.

Thus convex problem (P2.2), coupled with tuple $<\mathbf{p}^u, \mathbf{p}^d, \mathbf{R}^u>$, is expressed as

$$(P2.2) \quad \min_{\mathbf{p}^u, \mathbf{p}^d, \mathbf{R}^u} \sum_{i=1}^{K} L_i^u \frac{p_i^u}{R_i^u} + \sum_{i=1}^{K} \frac{C^3 (L_i - L_i^u)^3}{\left(\frac{L_i^u}{R_i^u}\right)^2}$$

$$+ \sum_{j=1}^{K} \gamma L_i^u \frac{p_j^d}{R_i^u} - \sum_{j=1}^{K} \beta f(p_j^d) \gamma \frac{L_i^u}{R_i^u}$$

$$s.t. \begin{cases} \sum_{i=1}^{K} L_i^u \frac{p_i^u}{R_i^u} + \sum_{i=1}^{K} \frac{C^3 (L_i - L_i^u)^3}{\left(\frac{L_i^u}{R_i^u}\right)^2} \\ \leq \sum_{j=1}^{K} \beta f(p_j^d) \gamma \frac{L_i^u}{R_i^u} \\ 0 \leq L_i^u \leq L_i \\ 0 \leq R_i^u \leq R_{i,max}^u \\ P_{min}^u \leq p_i^u \leq P_{max}^u \\ P_{min}^d \leq p_j^d \leq P_{max}^d \\ 0 \leq \frac{L_i^u}{R_i^u} \leq T \end{cases} \qquad (28)$$

where $L_i^u, i \in \{1, ..., K\}$ is fixed.

Proof: Let $v_i = \frac{1}{R_i^u}$ and $q_i = (R_i^u)^2$, we can obtain an optimal model with five variables as described below

$$(P2.3) \quad \min_{\mathbf{p}^u, \mathbf{p}^d, \mathbf{R}^u, \mathbf{v}, \mathbf{q}} \sum_{i=1}^{K} L_i^u p_i^u v_i + \sum_{i=1}^{K} \frac{C^3 (L_i - L_i^u)^3}{(L_i^u)^2} q_i$$

$$+ \sum_{j=1}^{K} \gamma L_i^u p_j^d v_i - \sum_{j=1}^{K} \beta f(p_j^d) \gamma L_i^u v_i$$

$$s.t. \begin{cases} \sum_{i=1}^{K} L_i^u p_i^u v_i + \sum_{i=1}^{K} \frac{C^3 (L_i - L_i^u)^3}{(L_i^u)^2} q_i \\ \leq \sum_{j=1}^{K} \beta f(p_j^d) \gamma L_i^u v_i \\ 0 \leq L_i^u \leq L_i \\ 0 \leq R_i^u \leq R_{i,max}^u \\ P_{min}^u \leq p_i^u \leq P_{max}^u \\ P_{min}^d \leq p_j^d \leq P_{max}^d \\ 0 \leq L_i^u v_i \leq T \end{cases} \qquad (29)$$

where, $\mathbf{v} = [v_1, v_2, ..., v_K], \mathbf{q} = [q_1, q_2, ..., q_K]$.

For problem (P2.3), the second-order derivative of each variable in the objective function equals zero. In addition, all

constraints are linear. Therefore, problem (P2.2) is a convex optimization problem that can be solved using standard interior point algorithm.

We continue to optimize the second set of variables $\langle \mathbf{L}^u, \mathbf{R}^u \rangle$ with fixed variables $\mathbf{p}^u, \mathbf{p}^d$. Problem (P2.2) is then transformed to the following

$$(P3) \quad \min_{\mathbf{L}^u, \mathbf{R}^u} \sum_{i=1}^{K} L_i^u \frac{p_i^u}{R_i^u} + \sum_{i=1}^{K} \frac{C^3 (L_i - L_i^u)^3}{\left(\frac{L_i^u}{R_i^u}\right)^2}$$
$$+ \sum_{j=1}^{K} \gamma L_i^u \frac{p_j^d}{R_i^u} - \sum_{j=1}^{K} \beta f(p_j^d) \gamma \frac{L_i^u}{R_i^u}$$

$$s.t. \begin{cases} \sum_{i=1}^{K} L_i^u \frac{p_i^u}{R_i^u} + \sum_{i=1}^{K} \frac{C^3 (L_i - L_i^u)^3}{\left(\frac{L_i^u}{R_i^u}\right)^2} \\ \leq \sum_{j=1}^{K} \beta f(p_j^d) \gamma \frac{L_i^u}{R_i^u} \\ 0 \leq L_i^u \leq L_i \\ 0 \leq R_i^u \leq R_{i,max}^u \\ P_{min}^u \leq p_i^u \leq P_{max}^u \\ P_{min}^d \leq p_j^d \leq P_{max}^d \\ 0 \leq \frac{L_i^u}{R_i^u} \leq T \end{cases} \quad (30)$$

where $p_i^u, p_j^d, i \in \{1, \dots, K\}, j \in \{1, \dots, K\}$ are fixed, and the problem (P3) is also convex.

Proof: Let $v_i = \frac{1}{R_i^u}, q_i = (R_i^u)^2, e_i = \frac{1}{L_i^u}, x_i = \frac{1}{(L_i^u)^2}$, and consider the following problem comprising of four variables

$$(P3.1) \quad \min_{\mathbf{L}^u, \mathbf{v}, \mathbf{q}, \mathbf{e}, \mathbf{x}} \sum_{i=1}^{K} p_i^u L_i^u v_i + \sum_{j=1}^{K} \gamma p_j^d L_i^u v_i$$
$$+ \sum_{i=1}^{K} \Lambda - \sum_{j=1}^{K} \beta f(p_j^d) \gamma L_i^u v_i$$

$$s.t. \begin{cases} \sum_{i=1}^{K} L_i^u p_i^u v_i + \sum_{i=1}^{K} \Lambda \\ \leq \sum_{j=1}^{K} \beta f(p_j^d) \gamma L_i^u v_i \\ 0 \leq L_i^u \leq L_i \\ 0 \leq R_i^u \leq R_{i,max}^u \\ P_{min}^u \leq p_i^u \leq P_{max}^u \\ P_{min}^d \leq p_j^d \leq P_{max}^d \\ 0 \leq L_i^u v_i \leq T \end{cases} \quad (31)$$

where $\mathbf{v} = [v_1, v_2, \dots, v_K]$, $\mathbf{q} = [q_1, q_2, \dots, q_K]$, $\mathbf{e} = [e_1, e_2, \dots, e_K]$, $\mathbf{x} = [x_1, x_2, \dots, x_K]$, $\Lambda = \frac{C^3}{\gamma^2}(L_i^3 x - 3L_i^2 e - L_i^u + 3L_i)q_i$.

We determine the second derivative of each variable in the objective function of (P3.1). Again, the second-order derivative is zero, which proves that the objective function is convex. The constraints also indicate convexity. We use the interior point algorithm to obtain the final optimal solution.

Based on the above characteristics, we propose an algorithm to effectively solve subproblem (P2), with the main steps summarized in **Algorithm 2**.

Algorithm 2 Group Iterative Optimization

Input: $K, M, B, \mathbf{H}^u, \mathbf{H}^d, \mathbf{H}_0, T, C, \kappa, \beta, \gamma, \mathbf{L}, \delta_j^2, \delta_B^2, \mathbf{s}^u,$
    $\mathbf{s}^d, P_{min}^u, P_{max}^u, P_{min}^d, P_{max}^d, \mathbf{L}^{u(0)}, \mathbf{p}^{u(0)}, \mathbf{p}^{d(0)}, \mathbf{R}^{u(0)}$
1: Set the initial value $\mathbf{L}_{ini}^u = \mathbf{L}^{u(0)}, \mathbf{p}_{ini}^u = \mathbf{p}^{u(0)}, \mathbf{p}_{ini}^d =$
    $\mathbf{p}^{d(0)}, \mathbf{R}_{ini}^u = \mathbf{R}^{u(0)}$, and iteration number $n = 1$
2: **repeat**
3:     Solve problem (P2.2) with fixed $\mathbf{L}^{u(n-1)}$, while $\mathbf{p}_{ini}^u =$
       $\mathbf{p}^{u(n-1)}, \mathbf{p}_{ini}^d = \mathbf{p}^{d(n-1)}, \mathbf{R}_{ini}^u = \mathbf{R}^{u(n-1)}$, to achieve the
       optimal $(\mathbf{p}^{u(n)}, \mathbf{p}^{d(n)}, \mathbf{R}^{u(n)})$;
4:     Solve problem (P3) with fixed $(\mathbf{p}^{u(n)}, \mathbf{p}^{d(n)})$, while
       $\mathbf{R}_{ini}^u = \mathbf{R}^{u(n)}$, to achieve the optimal $(\mathbf{L}^{u(n)}, \mathbf{R}^{u(n)})$
5:     Set $n = n + 1$;
6: **until** the cost function of problem (P2) convergences.
Output: $\mathbf{L}_{opt}^u, \mathbf{p}_{opt}^u, \mathbf{p}_{opt}^d, \mathbf{R}_{opt}^u$

V. NUMERICAL RESULTS

In this section we present the numerical results in order to demonstrate the superiority of the proposed algorithm. For comparisons, we propose two benchmark schemes:

1) ***The fixed-variable scheme***, whereby variables $\mathbf{p}^u, \mathbf{p}^d, \mathbf{L}^u$, and $\mathbf{R}^u$ are fixed on their initial values, i.e.,

$$\mathbf{L}^u = \mathbf{L}_{ini}^u = \theta \mathbf{L}, \quad (32)$$
$$\mathbf{p}^u = \mathbf{p}_{ini}^u, \quad (33)$$
$$\mathbf{p}^d = \mathbf{p}_{ini}^d, \quad (34)$$
$$\mathbf{R}^u = \mathbf{R}_{ini}^u = \mathbf{R}_{max}^u, \quad (35)$$

where $0 \leq \theta \leq 1$ is the offloading ratio.

2) ***The full-offloading scheme***, whereby all users upload their total computation tasks to the BS. Thus, no local computation is required and the optimal CPU frequency of local compution equals zero. By solving problems (P2.2) and (P3), the optimal transmitted power $(\mathbf{p}_{opt}^u, \mathbf{p}_{opt}^d)$ and the optimal transmission rate $(\mathbf{R}_{opt}^u)$ can be obtained with $\mathbf{L}^u = \mathbf{L}$, $\mathbf{f}^{opt} = [0, 0, \dots, 0]$.

The simulation parameters are summarized in Table 1. For accuracy, we run over 1000 Monte-Carlo simulations to average the optimization results.

Fig. 3 demonstrates that the proposed algorithm converges after four runs under varying computation task sizes. This indicates the effectiveness of the proposed algorithm. Fig. 4 presents the average energy consumption of the system versus computation task size $\mathbf{L}$ when $K = 2$ and $M = 6$. The average energy consumption increases with computation task size $\mathbf{L}$ under all scenarios. For the fixed-variable scheme, it is seen when θ increases from 0.1 to 1, more offloading tasks cause more energy consumption. Moreover, the proposed algorithm is superior to the two benchmark schemes, the fixed-variable scheme and the full-offloading scheme. In addition, it is clear that the full-offloading scheme which includes power allocation optimization achieves a

TABLE 1. Simulation parameters.

Parameter	Value
Number of users, K	$2-6$
Number of antenna, M	$1, 4, 6, 8$
Channel matrix, $\mathbf{H}^u, \mathbf{H}^d, \mathbf{H}_0$	Modeled as Random Raylaigh Fading channel$\sim \mathcal{CN}(0, 0.01)$
Minimum transmitted power of users, P^u_{min}	$1W$
Maximum transmitted power of users, P^u_{max}	$5W$
Minimum transmitted power of BS, P^d_{min}	$5W$
Maximum transmitted power of BS, P^d_{max}	$25W$
AWGN power, $\delta^2_B = \delta^2_j$	$10^{-7}W$
Bandwidth	$2MHz$
PS receiver parameter, β	0.7
Chip effective capacitance coefficient, κ	10^{-28}
CPU cycles, C	$10^3 cycles/bit$
weight factor, θ, γ	$\theta = 0.1, \gamma = 1$

FIGURE 3. Convergence behavior of the proposed algorithm.

FIGURE 4. The sum energy consumption of the system versus the computation task size L.

much better performance compared to the fixed-variable scheme which excludes power allocation optimization. This implies that power allocation optimization results in greater improvements to system performance.
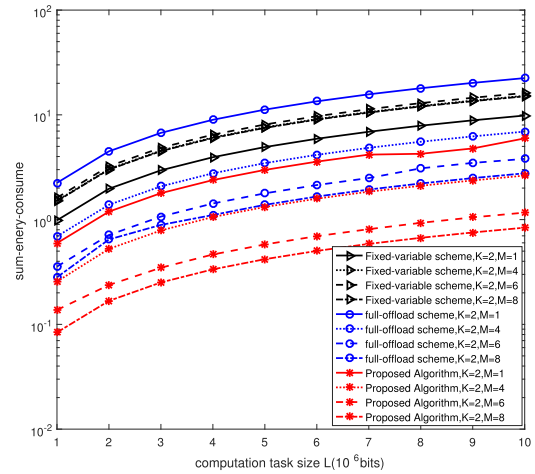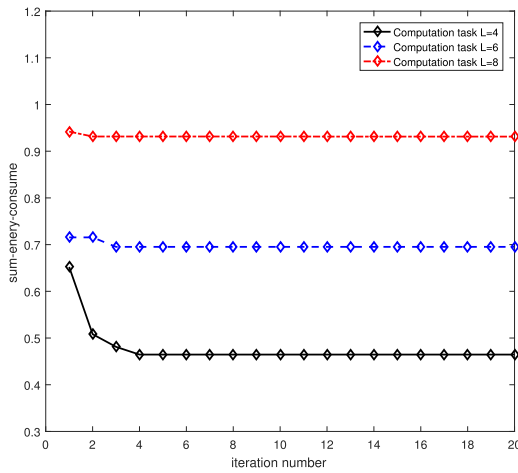

FIGURE 5. The sum energy consumption of the system versus the computation task size **L** under different number of BS antennas (*M*).
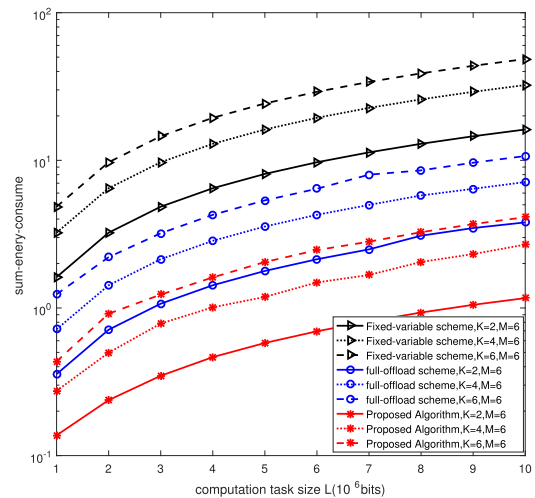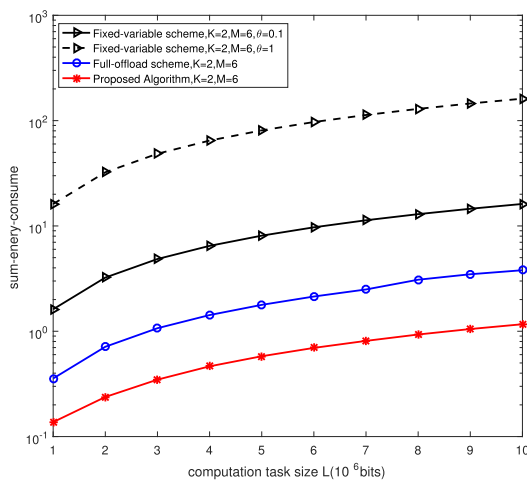

FIGURE 6. The sum energy consumption of the system versus the computation task size **L** under different number of users (*K*).

Fig. 5 compares the system energy consumption versus computation task size **L** under different number of the BS antennas M. For the fixed-variable scheme, the number of antennas has least influence on energy consumption. However, for the full-offloading scheme and our proposed algorithm, the system energy consumption is greatly reduced when $M = 8$ compared with $M = 1$ scenario. Thus, as the number of the BS antennas increases, our algorithm exhibits greater decline in energy consumption. As a result, we conclude that a greater amount of BS antennas will provide an improved system performance for our system.

Fig. 6 shows that the total energy consumption increases with number of users K under different computation task sizes. This can be attributed to more offloading data when the number of users increases, resulting in higher energy consumption of the system. In addition, the proposed algorithm performs the best in energy consumption compared with the other two schemes, demonstrating the suitability of the proposed algorithm in multi-user senarios.
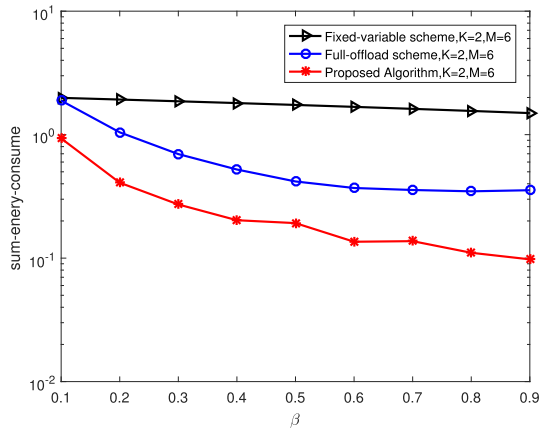
FIGURE 7. The sum energy consumption of the system versus PS receiver coefficient β.
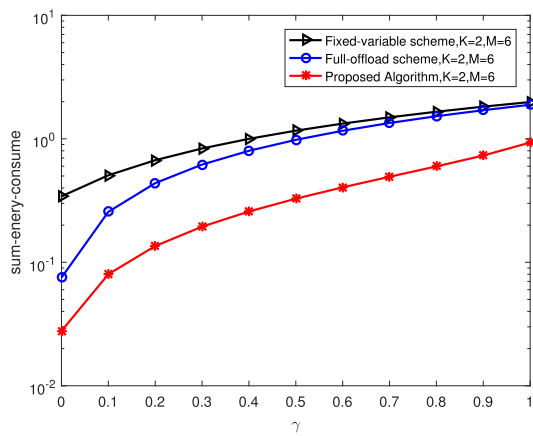

FIGURE 8. The sum energy consumption of the system versus the downlink time weight factor γ.

FIGURE 9. The offloading delay versus the computation task size **L**.

VI. CONCLUSION

We investigated a novel resource allocation model that combined MEC and SWIPT technologies for a MIMO FD-enabled cellular communication system to reduce the burden of users' intensive computation tasks and the energy consumption of the multi-user FD-MEC cellular network. We formulate a jointly optimization problem for CPU frequency, transmitted power, transmission rate, and offloading computation size. Furthermore, we decomposed the original problem into two subproblems, and the group iterative optimization algorithm was proposed to solve these problems. Numerical results demonstrate that our optimization scheme converges to the optimal solution within a minimal number of iterations and clearly outperforms the current baseline schemes both in energy consumption and latency.

Fig. 7 compares the energy consumption of the three schemes under different PS receiver coefficient β. The energy consumption decreases with β in all three schemes. This is because β represents the users' capability of energy harvesting. When β increases, it means more harvested energy, in other words users can consume less of their own energy to finish the computing tasks. The relations between the system energy consumption and the downlink time weight factor γ is illustrated in Fig. 8. It is clear that the sum energy consumption increases with γ. This implies that it is beneficial to decrease the downlink transmission time such that the system energy consumption will be reduced.

Fig.9 illustrates the offloading delay of the uplink users for the three schemes. The fixed-variable scheme shows a small superiority than the full-offloading scheme because the simulation of the fixed-variable scheme runs at the offloading ratio $\theta = 0.1$, which means smaller offloading task than the full-offloading scheme. The proposed algorithm shows the best latency performance among the three schemes which indicates the great advantage of our scheme not only in the energy efficiency but also in the latency performance.
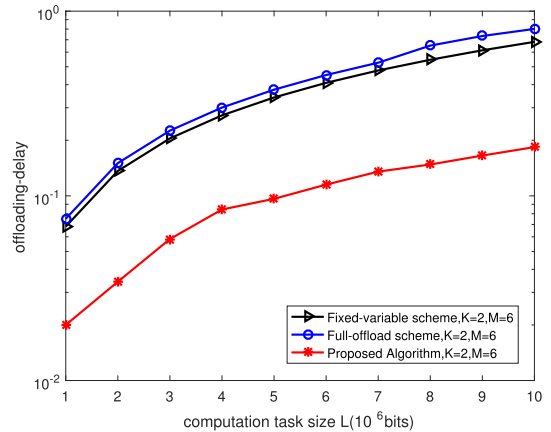
REFERENCES

[1] Z. Tang, J. Li, J. Abdoli, and Z. Guo, "Soft air interface to support 5G services and requirements," *Proc. IEEE 87th Veh. Technol. Conf. (VTC Spring)*, Porto, Portugal, Jun. 2018, pp. 1–6.

[2] A. Santoyo-González and C. Cervelló-Pastor, "Edge nodes infrastructure placement parameters for 5G networks," in *Proc. IEEE Conf. Standards Commun. Netw. (CSCN)*, Paris, France, Oct. 2018, pp. 1–6.

[3] Z. Ding, P. Ren, and Q. Du, "Mobility based routing protocol with MAC collision improvement in vehicular ad hoc networks," in *Proc. IEEE Int. Conf. Commun. Workshops (ICC Workshops)*, Kansas City, MO, USA, May 2018, pp. 1–6.

[4] A. Gupta and E. R. K. Jha, "A survey of 5G network: Architecture and emerging technologies," *IEEE Access*, vol. 3, pp. 1206–1232, Jul. 2015.

[5] R. Ma, G. Liu, Q. Hao, and C. Wang, "Smart microphone array design for speech enhancement in financial VR and AR," in *Proc. IEEE SENSORS*, Glasgow, U.K., Oct./Nov. 2017, pp. 1–3.

[6] J. Carneiro, R. J. F. Rossetti, D. C. Silva, and E. C. Oliveira, "BIM, GIS, IoT, and AR/VR integration for smart maintenance and management of road networks: A review," in *Proc. IEEE Int. Smart Cities Conf. (ISC)*, Kansas City, MO, USA, Sep. 2018, pp. 1–7.

[7] M. A. Farahani and K. Yamamoto, "Development of AR/VR navigation system using non-linguistic information," in *Proc. 11th Int. Conf. Comput. Sci. Educ. (ICCSE)*, Nagoya, Japan, Aug. 2016, pp. 332–337.

[8] M. Baz, "A collaborative energy optimization routing metric for IoT network over smart city," in *Proc. 1st Int. Conf. Comput. Appl. Inf. Secur. (ICCAIS)*, Riyadh, Saudi Arabia, Apr. 2018, pp. 1–7.

[9] R. Dagar, S. Som, and S. K. Khatri, "Smart farming—IoT in agriculture," in *Proc. Int. Conf. Inventive Res. Comput. Appl. (ICIRCA)*, Coimbatore, India, 2018, pp. 1052–1056.

[10] V. P. Mishra and A. Chaudhry, "The role of information and communication technologies in architecture and planning with vertical farming," in *Proc. Amity Int. Conf. Artif. Intell. (AICAI)*, Dubai, United Arab Emirates, Feb. 2019, pp. 1–3.

[11] H. Ahn, J. Lee, C. Kim, and Y.-J. Suh, "Frequency domain coordination MAC protocol for full-duplex wireless networks," *IEEE Commun. Lett.*, vol. 23, no. 3, pp. 518–521, Mar. 2019.

[12] D. Kim, H. Lee, and D. Hong, "A survey of in-band full-duplex transmission: From the perspective of PHY and MAC layers," *IEEE Commun. Surveys Tuts.*, vol. 17, no. 4, pp. 2017–2046, 4th Quart., 2015.

[13] A. Sabharwal, P. Schniter, D. Guo, D. W. Bliss, S. Rangarajan, and R. Wichman, "In-band full-duplex wireless: Challenges and opportunities," *IEEE J. Sel. Areas Commun.*, vol. 32, no. 9, pp. 1637–1652, Sep. 2014.

[14] J. Zhou, T.-H. Chuang, T. Dinc, and H. Krishnaswamy, "Integrated wideband self-interference cancellation in the RF domain for FDD and full-duplex wireless," *IEEE J. Solid-State Circuits*, vol. 50, no. 12, pp. 3015–3031, Dec. 2015.

[15] D. Liu, B. Zhao, F. Wu, S. Shao, X. Pu, and Y. Tang, "Semi-blind SI cancellation for in-band full-duplex wireless communications," *IEEE Commun. Lett.*, vol. 22, no. 5, pp. 1078–1081, May 2018.

[16] V. Tapio, H. Alves, and M. Juntti, "Joint analog and digital self-interference cancellation and full-duplex system performance," in *Proc. IEEE Int. Conf. Acoust., Speech Signal Process. (ICASSP)*, New Orleans, LA, USA, Mar. 2017, pp. 6553–6557.

[17] S. Dang, G. Chen, and J. P. Coon, "Outage performance analysis of full-duplex relay-assisted device-to-device systems in uplink cellular networks," *IEEE Trans. Veh. Technol.*, vol. 66, no. 5, pp. 4506–4510, May 2017.

[18] Q. Zeng, B. Zhong, J. Sun, C. Liu, and M. Wang, "Full-duplex relay aided device-to-device communication networks under the coverage of unmanned aerial vehicle base station," in *Proc. 24th Asia–Pacific Conf. Commun. (APCC)*, Ningbo, China, Nov. 2018, pp. 196–200.

[19] F. Chen, J. Hua, Z. Wang, Y. Zhou, and W. Qiu, "Joint user pairing and power allocation for full-duplex MIMO cellular systems under imperfect channel state information," in *Proc. 10th Int. Conf. Wireless Commun. Signal Process. (WCSP)*, Hangzhou, China, Oct. 2018, pp. 1–6.

[20] Y. Mao, C. You, J. Zhang, K. Huang, and K. B. Letaief, "A survey on mobile edge computing: The communication perspective," *IEEE Commun. Surveys Tuts.*, vol. 19, no. 4, pp. 2322–2358, 4th Quart., 2017.

[21] P. Mach and Z. Becvar, "Mobile edge computing: A survey on architecture and computation offloading," *IEEE Commun. Surveys Tuts.*, vol. 19, no. 3, pp. 1628–1656, 3rd Quart., 2017.

[22] H. Zhang, Y.-X. Guo, Z. Zhong, and W. Wu, "Cooperative integration of RF energy harvesting and dedicated WPT for wireless sensor networks," *IEEE Microw. Wireless Compon. Lett.*, vol. 29, no. 4, pp. 291–293, Apr. 2019.

[23] L. R. Varshney, "Transporting information and energy simultaneously," in *Proc. IEEE Int. Symp. Inf. Theory*, Toronto, ON, Canada, Jul. 2008, pp. 1612–1616.

[24] S. Gao, K. Xiong, R. Jiang, L. Zhou, and H. Tang, "Outage performance of wireless-powered SWIPT networks with non-linear EH model in Nakagami-m fading," in *Proc. 14th IEEE Int. Conf. Signal Process. (ICSP)*, Beijing, China, Aug. 2018, pp. 668–671.

[25] J. Li, F. Liu, and C. Guo, "A polarization-based power-splitting full-duplex relaying scheme design for SWIPT system," in *Proc. Asia–Pacific Microw. Conf. (APMC)*, Kyoto, Japan, Nov. 2018, pp. 1441–1443.

[26] R. Jiang, K. Xiong, P. Fan, Y. Zhang, and Z. Zhong, "Power minimization in SWIPT networks with coexisting power-splitting and time-switching users under nonlinear EH model," *IEEE Internet Things J.*, vol. 6, no. 5, pp. 8853–8869, Oct. 2019.

[27] S. Biswas, K. Singh, O. Taghizadeh, and T. Ratnarajah, "Coexistence of MIMO radar and FD MIMO cellular systems with QoS considerations," *IEEE Trans. Wireless Commun.*, vol. 17, no. 11, pp. 7281–7294, Nov. 2018.

[28] Z. Yang, J. Hou, and M. Shikh-Bahaei, "Resource allocation in full-duplex mobile-edge computation systems with NOMA and energy harvesting," in *Proc. IEEE Int. Conf. Commun. (ICC)*, Shanghai, China, May 2019, pp. 1–6.

[29] S. Mao, S. Leng, K. Yang, X. Huang, and Q. Zhao, "Fair energy-efficient scheduling in wireless powered full-duplex mobile-edge computing systems," in *Proc. IEEE Global Commun. Conf. (GLOBALCOM)*, Singapore, Dec. 2017, pp. 1–6.

[30] Z. Wen, K. Yang, X. Liu, S. Li, and J. Zou, "Joint offloading and computing design in wireless powered mobile-edge computing systems with full-duplex relaying," *IEEE Access*, vol. 6, pp. 72786–72795, 2018.

[31] H. Li, G. Shou, Y. Hu, and Z. Guo, "Mobile edge computing: Progress and challenges," in *Proc. 4th IEEE Int. Conf. Mobile Cloud Comput., Services, Eng. (MobileCloud)*, Oxford, U.K., Mar./Apr. 2016, pp. 83–84.

[32] F. Guo, L. Ma, H. Zhang, H. Ji, and X. Li, "Joint load management and resource allocation in the energy harvesting powered small cell networks with mobile edge computing," in *Proc. IEEE Conf. Comput. Commun. Workshops (INFOCOM WKSHPS)*, Honolulu, HI, USA, Apr. 2018, pp. 299–304.

[33] G. Zhang, W. Zhang, Y. Cao, D. Li, and L. Wang, "Energy-delay tradeoff for dynamic offloading in mobile-edge computing system with energy harvesting devices," *IEEE Trans. Ind. Informat.*, vol. 14, no. 10, pp. 4642–4655, Oct. 2018.

[34] G. Zhang, Y. Chen, Z. Shen, and L. Wang, "Distributed energy management for multiuser mobile-edge computing systems with energy harvesting devices and QoS constraints," *IEEE Internet Things J.*, vol. 6, no. 3, pp. 4035–4048, Jun. 2019.

[35] J. Zeng, T. Lv, R. P. Liu, X. Su, M. Peng, C. Wang, and J. Mei, "Investigation on evolving single-carrier NOMA into multi-carrier NOMA in 5G," *IEEE Access*, vol. 6, pp. 48268–48288, 2018.

[36] Z. Ding, J. Xu, O. A. Dobre, and H. V. Poor, "Joint power and time allocation for NOMA–MEC offloading," *IEEE Trans. Veh. Technol.*, vol. 68, no. 6, pp. 6207–6211, Jun. 2019.

[37] Y. Pan, M. Chen, Z. Yang, N. Huang, and M. Shikh-Bahaei, "Energy-efficient NOMA-based mobile edge computing offloading," *IEEE Commun. Lett.*, vol. 23, no. 2, pp. 310–313, Feb. 2019.

[38] R. Y. Beltran and M. Eaton, "Efficient applications of bus transfer schemes utilizing microprocessor based relaying technology," in *Proc. 62nd Annu. Conf. Protective Relay Eng.*, Austin, TX, USA, Mar./Apr. 2009, pp. 469–474.

[39] Z. Tan, F. R. Yu, X. Li, H. Ji, and V. C. M. Leung, "Virtual resource allocation for heterogeneous services in full duplex-enabled SCNs with mobile edge computing and caching," *IEEE Trans. Veh. Technol.*, vol. 67, no. 2, pp. 1794–1808, Feb. 2018.

[40] M. Liu, Y. Mao, S. Leng, and S. Mao, "Full-duplex aided user virtualization for mobile edge computing in 5G networks," *IEEE Access*, vol. 6, pp. 2996–3007, 2017.

[41] K. Li, M. Tao, and Z. Chen, "Exploiting computation replication for mobile edge computing: A fundamental computation-communication tradeoff study," 2019, *arXiv:1903.10837*. [Online]. Available: https://arxiv.org/abs/1903.10837

[42] S. Bi and Y. Zhang, "Computation rate maximization for wireless powered mobile-edge computing with binary computation offloading," *IEEE Trans. Wireless Commun.*, vol. 17, no. 6, pp. 4177–4190, Jun. 2018.

[43] X. Cao, F. Wang, J. Xu, R. Zhang, and S. Cui, "Joint computation and communication cooperation for energy-efficient mobile edge computing," *IEEE Internet Things J.*, vol. 6, no. 3, pp. 4188–4200, Jun. 2019.

[44] W. Feng, J. Xu, and Z. Ding, "Multi-antenna NOMA for computation offloading in multiuser mobile edge computing systems," *IEEE Trans. Commun*, vol. 67, no. 3, pp. 2450–2463, Mar. 2019.

[45] F. Wang, J. Xu, X. Wang, and S. Cui, "Joint offloading and computing optimization in wireless powered mobile-edge computing systems," *IEEE Trans. Wireless Commun.*, vol. 17, no. 3, pp. 1784–1797, Mar. 2018.

[46] D. Li, C. Shen, and Z. Qiu, "Two-way relay beamforming for sum-rate maximization and energy harvesting," in *Proc. IEEE Int. Conf. Commun. (ICC)*, Budapest, Hungary, Jun. 2013, pp. 3115–3120.

[47] Y. Mao, J. Zhang, Z. Chen, and K. B. Letaief, "Dynamic computation offloading for mobile-edge computing with energy harvesting devices," *IEEE J. Sel. Areas Commun.*, vol. 34, no. 12, pp. 3590–3605, Dec. 2016.
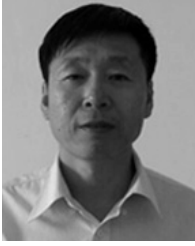
FANGNI CHEN received the B.S. degree in communication engineering and the Ph.D. degree in information and communication engineering from Zhejiang University, China, in 2003 and 2008, respectively. She has been an Assistant Professor with the School of Information and Electronic Engineering, Zhejiang University of Science and Technology, China, since 2008. She has been a Postdoctoral Research Fellow with the College of Information Engineering, Zhejiang University of Technology, China, since 2018. Her research interests include LDPC code, full-duplex technology, mobile edge computing, and deep learning.

JIAFEI FU received the B.S. degree in information engineering from Lishui University, Zhejiang, China. She is currently pursuing the M.S. degree in information engineering with the Zhejiang University of Technology. Her research interests include wireless location, full-duplex, and mobile edge computing.

ZHONGPENG WANG received the B.S. degree in microelectronic technique from Liaoning University, Shenyang, China, in 1988, the M.S. degree in microelectronic technique from the Harbin Institute of Technology, Harbin, China, in 1995, and the Ph.D. degree from the Beijing University of Posts and Telecommunications, Beijing, China, in 2004. He is currently working with the Zhejiang University of Science and Technology, China. He is also with the State Key Laboratory of Millimeter Waves, Southeast University, Nanjing, China. His research interests include physical layer security, 5G/6G wireless communications, visible light communications, and MIMO wireless communications.

YANG ZHOU received the B.S. degree in electronic information engineering from Zhejiang Normal University, Jinhua, Zhejiang, in 2006, the M.S. degree in communication and information system from Beihang University, Beijing, in 2009, and the Ph.D. degree in measuring and testing technologies and instruments from the University of Shanghai for Science and Technology, Shanghai, in 2013. He is currently an Assistant Professor with the School of Information and Electronic Engineering, Zhejiang University of Science and Technology, China. His research interests include the image processing and biological/medical imaging techniques using OCT device.

WEIWEI QIU received the B.S. degree in electrical engineering and information science and the Ph.D. degree in electrical science and technology engineering from the University of Science and Technology of China, Hefei, in 2007 and 2013, respectively. Since 2013, she has been an Assistant Professor with the School of Information and Electronic Engineering, Zhejiang University of Science and Technology. Her research interests include optical fiber communication and sub-system research.

● ● ●